REMOTE CONTROL OF A CYBORG MOTH USING CARBON NANOTUBE-ENHANCED FLEXIBLE NEUROPROSTHETIC PROBE

W.M. Tsang[1], A. Stone[2], Z. Aldworth[3], D. Otten[1], A.I. Akinwande[1], T. Daniel[3], J.G. Hildebrand[2], R.B. Levine[2], J. Voldman[1]
[1]Massachusetts Institute of Technology, Cambridge, MA, USA
[2]University of Arizona, Tucson, AZ, USA
[3]University of Washington, Seattle, WA, USA

ABSTRACT

We report the first remote flight control of an insect using microfabricated flexible neuroprosthetic probes (FNPs) that directly interface with the animal's central nervous system. The FNPs have a novel split-ring design that incorporates the anatomical bi-cylinder structure of the nerve cord and allows for an efficient surgical process for implantation (Figure 1a). Additionally, we have integrated carbon nanotube (CNT)-Au nanocomposites into the FNPs to enhance the charge injection capability of the probe. The FNPs integrated with a wireless system are able to evoke multi-directional, graded abdominal motions in the moths thus altering their flight path.

1. INTRODUCTION

There is considerable interest in creating insect-based Micro-Air-Vehicles (i-MAVs) that would combine the advantageous features of insects—small size, effective energy storage, navigation ability—with the benefits of MEMS and electronics—sensing, actuation and information processing. The two basic components of the i-MAV are the telemetry system and the neuroprosthetic probe (Figure 1c). The telemetry system provides a communication link between the insect and the base station, while the probe interfaces with the nervous system of the insect to bias the insect's flight path.

Several groups have developed telemetry systems that can be glued onto insects [1-4]. While microfabricated probes have been used to *record* the neural activity of insects [1], they have not been used to control them. Indeed, prior reports on the remote control of insects, including cockroaches [5], beetles [2] and moths [3, 4], have used thin metal wires for stimulation. Although remarkable results have been achieved with these systems, these metal wires do not offer the fine positional control and multisite stimulation capability provided by MEMS fabrication technology.

Here, we introduce microfabricated FNPs containing a split-ring structure that incorporates the anatomical bi-cylinder structure of the nerve cord of the moth *Manduca Sexta* (Figure 1a) to evoke the abdominal motions in the moths. Moreover, we have electroplated a CNT-Au nanocomposite film onto these FNPs to enhance the charge injection capability at the probe-neural interface and to reduce the stimulation voltage.

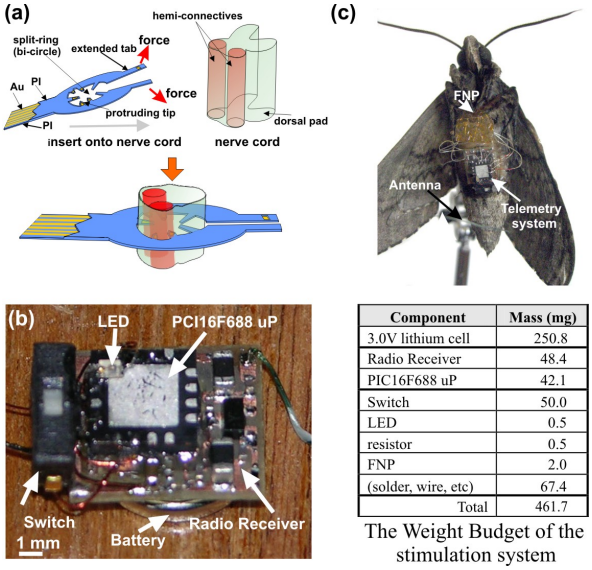

Component	Mass (mg)
3.0V lithium cell	250.8
Radio Receiver	48.4
PIC16F688 uP	42.1
Switch	50.0
LED	0.5
resistor	0.5
FNP	2.0
(solder, wire, etc)	67.4
Total	461.7

The Weight Budget of the stimulation system

Figure 1 (a) Schematic of the probe, showing the split-ring design that enables the probe to encircle the nerve cord. Images showing (b) the telemetry system and (c) a cyborg moth with FNP and telemetry system, along with a table describing the weight of the wireless system component.

We are able to elicit graded and multi-direction abdominal movements in both the pupae and adult moths using FNP stimulation. It is well known that insects maneuver their flight not only through rapid adjustments of their flapping wings, but also through flexing their abdomen to effect center-of-gravity shifts and consequently their flight attitude [6]. In this work, we have integrated the FNPs into a wireless system to alter flight path of the moth using the abdomen ruddering with FNP stimulation.

2. METHODS & RESULTS

Telemetry System

The telemetry system is assembled from commercially available devices and powered by a rechargeable battery (ML612S, Panasonic) (Figure 1b). The system has a single-channel AM receiver (microflierradio) to receive signals (27 MHz) from the transmitter and a microcontroller (PIC16F688, Microchip Technology) to generate the dipolar voltage pulses for the stimulations (6 channels). The dimensions and the

mass of the system are 6.8 mm × 10.2 mm × 5.1 mm and ~460 mg, respectively, which is small enough to be carried by most moths. The operating range and time of the system are ~10 m and ~3 hours, respectively, with a fully charged battery. While, the magnitude of the pulse is fixed to 3.0 V, the frequency and duration of the stimulation signal can be controlled via the transmitter. We connected the FNPs to the system using soldered Ag wires (Figure 1c).

Probe Design & Fabrication

The FNP is made of two layers of polyimide (PI) with gold sandwiched in-between in a split-ring geometry (Figure 1a). The main steps of FNPs fabrication are shown in Figure 2 and are previously reported [7]. Importantly, in this work we added an electroplating step to coat a CNT-Au nanocomposite onto the FNPs to reduce the impedance for charge conduction at the probe-neural interface. The coating is performed from an aqueous solution (1 mg/mL) consisting of multi-wall CNTs (Cheap Tubes Inc) mixed into a Au-electrolyte bath (TSG-250, Transene) with monophasic voltage pulses (1.0 V, 50% duty cycle, 1.5 min). The CNTs have a length of 0.5-2.0 µm and a diameter < 8 nm.

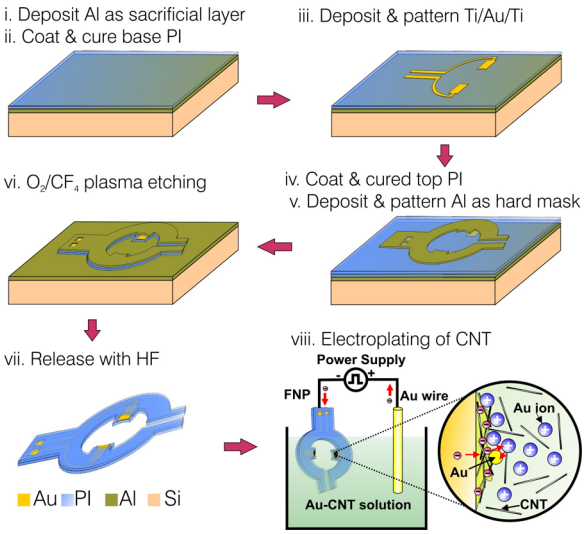

Figure 2: The fabrication process of CNT-Au enhanced FNPs.

Images of the fabricated FNPs are showed in Figure 3. They can be connected to the stimulator by either FFC\FPC connectors or metal wires with conductive epoxy. The FNPs show excellent flexibility (Figure 3a), allowing us to open the ring of the FNP during insertion around the nerve cord (Figure 1a). The two extended tabs at the tip of the FNP act as "handles" to manipulate the implant and lock the FNP in place after the insertion. As opposed to the initial FNP design (WH6, Figure 3b) [7] that assumed a cylindrical nerve cord structure, the new FNP designs (BC6 & BC8, Figure 3c-d) contain either 5 or 7 stimulation sites at the bottom of the split-ring in a bi-circle geometry. The bi-circle geometry allows multi-site stimulation that is anatomically matched to the insect nerve cord. Moreover, they have an additional stimulate site on the extended tab to act as a reference electrode (Figure 3a). In addition, the holding-tips at the top of the split-ring insert into the dorsal pad of the nerve cord to physically support the probe and prevent it from moving. The holding tips do not contain any stimulation sites in these new designs as there are no neuronal processes in the dorsal pad.

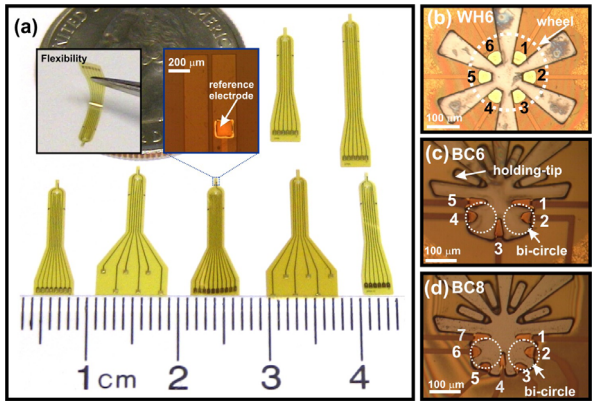

Figure 3: (a) Images for various FNP designs. Close-up images on the split-ring structure of the (b) WH6, (c) BC6, and (d) BC8 designs.

Probe Characterization

SEM images of the CNT-Au nanocomposite-coated FNPs (C-FNPs) show dense nano-protrusions on the surface of the stimulation sites (Figure 4a). Two characteristic peaks (the G-line peak at 1578 cm^{-1} and D-line peak at 1300 cm^{-1}), commonly observed in the multiwall CNTs [8], appear in the micro-Raman spectrum of C-FNPs at a laser excitation wavelength of 785 nm (HOLO LAB Series 5000).

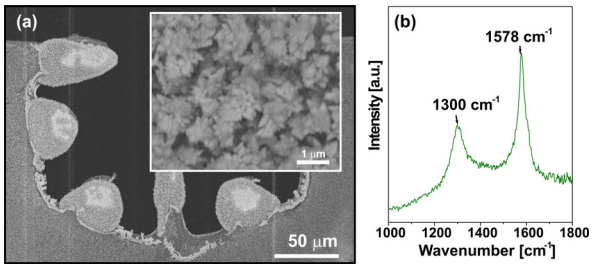

Figure 4: (a) The SEM images and (b) micro-Raman spectrum of C-FNP.

Electrical measurements of a representative FNP and C-FNP in saline solution using electrochemical impedance spectroscopy (EIS) are shown in Figure 5a along with a standard equivalent-circuit model for the probe. The measurements were taken between 1 Hz and 100 kHz using a 10 mV ac signal via a potentiostat (VersaSTAT3, AMETEK) with Pt wire as counter-electrode. In the model, the interface between

the probe and saline is represented by a constant phase element (CPE, with impedance $Z_{dl}=1/C_{dl}(j\omega)^n$) in parallel with the Faradic impedance R_f, while R_s is the spreading resistance of the solution. The charge injection capability of the probe is proportional to the value of C_{dl}.

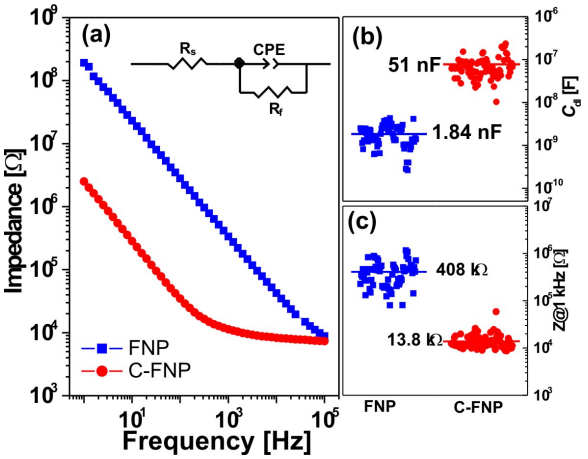

Figure 5: (a) The EIS spectra of a FNP and C-FNP. The extracted values of (b) C_{dl} and (c) interface impedance at 1 kHz from EIS.

The extracted values of C_{dl} increase from 1.84 nF to 51 nF following CNT-Au coating (Figure 5b) and the interfacial impedance at the biologically relevant frequency of 1 kHz decrease from 408 kΩ to 13.8 kΩ (Figure 5c), demonstrating that the interfacial properties of the probes are significantly improved (p<0.001, n=50 stimulation sites), which we attribute to the formation of the nano-protrusions. Moreover, *in vivo* characterization shows that the C-FNPs are able to elicit abdominal motion of the moths with a stimulation voltage significantly less (1.0 V vs. 2.0 V, p < 0.001, n=10 moths) than that of uncoated FNPs.

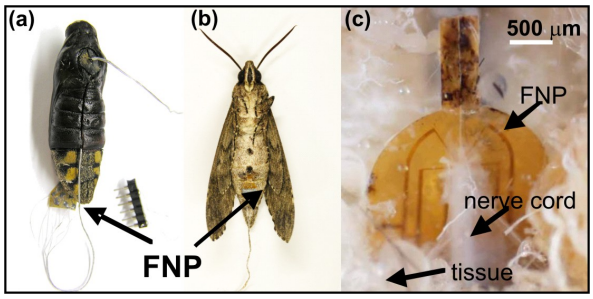

Figure 6: Images of (a) a pupa with inserted FNP; (b) eclosed adult moth with FNP inserted at the pupal stage and (c) image of dissected adult moth showing the growth of connective tissue around the nerve cord.

Implantation

We are able to implant the FNPs and C-FNPs into adult moths as well as pupal stages 12-17 (7-2 days prior to eclosion). The implantation is performed at the position of the ventral 4th abdominal segment for pupae and the ventral 1st abdominal segment for the adult moths, as previously reported [7]. Images of a pupa just after insertion of the FNP and after adult emergence are shown in Figure 6. Indeed, images of dissected adult moths with probes implanted in stage-16 pupae show tissue growth around the split-ring portion of the probe (Figure 6c) indicating the biocompatibility of the probe.

Neural Stimulation & Flight Control

We observed that stimulation of FNPs or C-FNPs could elicit multi-directional abdominal movements in both pupae (Figure 7) and adult moths (Figure 8). The directions of abdominal movement depend on the specific stimulation sites selected for stimulation (Figure 7a and b), and the magnitude of the movements increased with increases in either voltage magnitude or pulse frequency of the stimulation signal (Figure 7c and d).

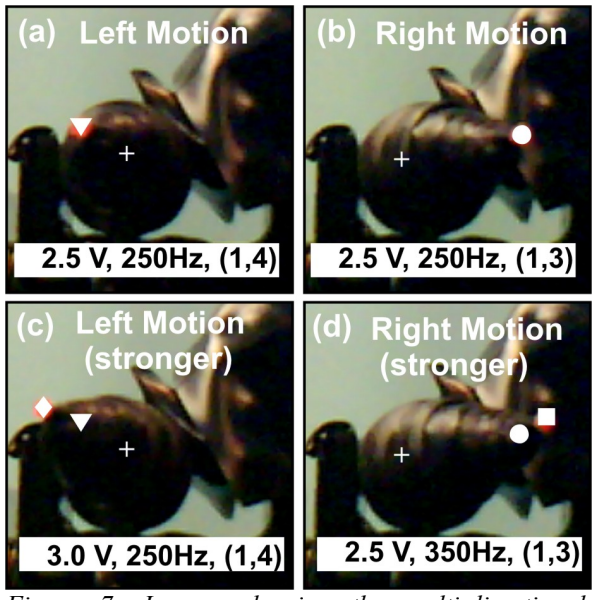

Figure 7: Images showing the multi-directional, graded abdominal movements at a pupa followed the C-FNP (BC8) stimulations. The location of the abdomen apex of the pupa before the stimulation is marked by '+' and has marked with other distinct symbols for each stimulation conditions. (a) Left ('▼') and (b) right ('●') abdomen movements achieved by applying the signal at the various site pairs of the probe. A stronger abdominal motion achieved with the increases in the (c) voltage ('◆') and the frequency ('■') of the stimulation signal.

Additionally, Figure 8 shows the results of the FNP (WH8) stimulation of an adult moth using our wireless system. Abdominal motions of a moth in the vertical (Figure 8a) and horizontal planes (Figure 8b) have been achieved with stimulations using various site pairs. Importantly, in the flight control experiment, we are able to force a freely flying animal to perform

turning motions (Figure 9a) using the abdominal ruddering with these elicited abdomen motions. These turning motions are well repeatable and the changes in the yaw angle of the moth with 4 successive stimulations are shown in Figure 9b.

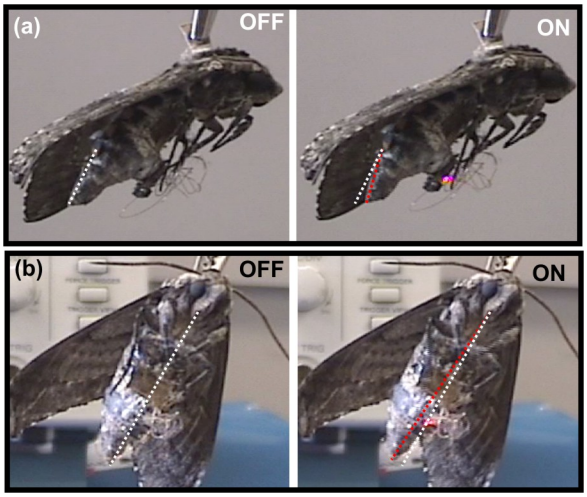

Figure 8: Images showing the abdominal motions of a moth in the (a) vertical and (b) horizontal planes elicited by the wireless microsystem using FNP stimulations with various pairs of stimulation sites.

Finally, we observed that the responses of animals were individually repeatable for successive stimulations (>10) during single developmental stage. However, the responses differed between animals and changed as the animal developed from pupa to adult. Differences across animals might reflect variation in the orientation of FNP relative to the nerve cord in different preparations, movement after implantation, or anatomical variability among insects.

3. CONCLUSION

We demonstrate the first remote flight control of moth using multisite neural stimulation on the central neural system of the moth with a microfabricated FNP. Furthermore, we show enhancement of the stimulation abilities of probe with a CNT-Au nanocomposite coating.

4. ACKNOWLEDGEMENT

This work was supported by the Air Force Research Laboratory as part of the DARPA HI-MEMS program. We thank the Microsystems Technology Laboratories for fabrication assistance. We thank Spencer Murray and Sam Sinai for assistance with FNP implantation, characterization and stimulation. We thank Jacob Armin Hinterwirth, Jacob Lockey and Billie Medina for assistance with wireless flight control experiments.

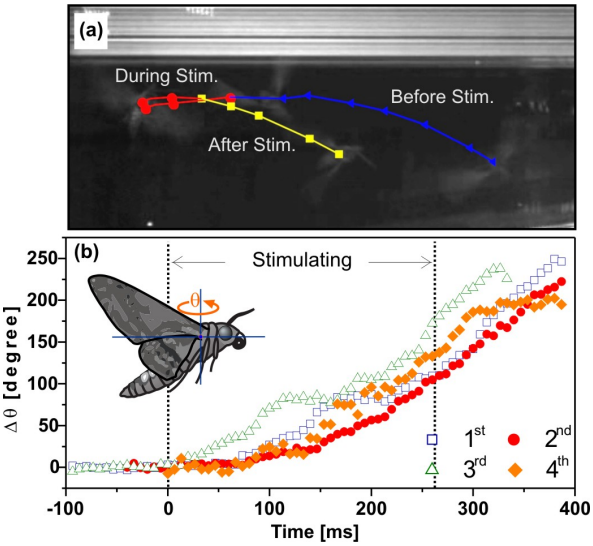

Figure 9: *(a) Side view image of a freely flying moth that has been stimulated to perform right turns following the elicited abdominal motions. The locations of the moth before, during and after the stimulation are marked by (▲), (●) and (■), respectively. (b) The changes of the yaw angle (θ) of the moth with 4 successive stimulations.*

REFERENCES

[1] S. Takeuchi and I. Shimoyama, "A Radio-Telemetry System with a Shape Memory Alloy Microelectrode for Neural Recording of Freely Moving Insects", IEEE Trans. Biomed. Eng. vol. 51, pp. 133-137, 2004

[2] H. Sato *et al*, "Radio-Controlled Beetles: A Radio-Frequency system for Insect Neural Flight Control", Proc. IEEE MEMS 2009, Sorrento, pp 216-219.

[3] A. Bozkurt *et al*,"Radio Control of Insects for Biobotic Domestication", Proc. IEEE NER 2009, Antalya, pp. 215-218.

[4] D.C. Daly *et al*, "A Pulsed Uwb Receiver Soc for Insect Motion Control", Proc. IEEE ISSCC2009, pp. 200-201.

[5] R. Holzer and I. Shimoyama, "Locomotion control of a bio-robotic system via electric stimulation", Proc. IEEE IROS 97, pp. 1514-1519.

[6] C.P. Ellington, "The aerodynamics of hovering insect flight", Philosophical Transactions of the Royal Society of London, B. Biological Sciences, vol. 305, pp. 1-181, 1984.

[7] W.M. Tsang *et al*, "Insect flight control by neural stimulation of pupae-implanted flexible multisite electrodes", Proc. MicroTAS '08, San Diego, pp.1922-1924.

[8] S.Y. Chen, "Fabrication and field emission property studies of multiwall carbon nanotubes" J. Phys. D: Appl. Phys. 37 273–279, 2004.